Half-Metallic Graphene Nanoribbons with SIESTA and Python

Nanometric System Simulation - Nanoscience and Nanotechnology UAB 2022/23

Xabier Oianguren Asua

In this practice, we replicate the results obtained by Soon et al. in Ref [1] using SIESTA [2, 3] and the `sisl` library [4] in python. The authors of the cited reference found by computational methods that a zigzag-shaped edge graphene nanoribbon (ZGNR) can change from being conductive to a half-metal behaviour just by placing a static electric field. A half-metal is a material where the states with one spin polarization have metallic behaviour while for the other spin polarization the behaviour is that of an insulator. All the scripts we employed for the present work can be found in the Github repository [5]. We implemented two main routines to automatize the SIESTA input file generation and simulation from Python. By varying their arguments, all the tasks for the present work were performed. These function can be found in Listing 2.

1 The Employed Geometry

We choose an 8 carbon wide ZGNR to check if we are able to quantitatively approach the results of the paper. For this, we employ as an initial ansatz geometry the one given by the ZGNR `sisl` function, as shown in Listing 1. We manually added to each side of the ribbon a hydrogen atom, since that is the way it is found in standard conditions. With this, we get the periodic cell shown in Figure 1. Due to the software implementation we must represent the ZGNR periodically in the three dimensions of space, even if we only care about the transport longitudinal direction x.

Listing 1: Generation of primitive cell.

```
import numpy as np
import sisl
import sisl.viz

width=8 # wisth of the nanoribbon
gnr=sisl.geom.graphene_nanoribbon(width=width, bond=1.42, atoms=None, kind='zigzag')
edgeC_idxs=[0,7] # the Carbons in the edges have these indices
CH=CH = 1.09 #A Benzene distance from C to H
h_atoms = sisl.Geometry(np.array([gnr.axyz()[edgeC_idxs[0]]-np.array([0,CH,0]),
                                  gnr.axyz()[edgeC_idxs[1]]+np.array([0,CH,0])  ]),
          [sisl.Atom('H'), sisl.Atom('H')])
gnr=gnr.insert(-1, h_atoms)
gnr.plot(axes="xy") # Generates Figure 1
```

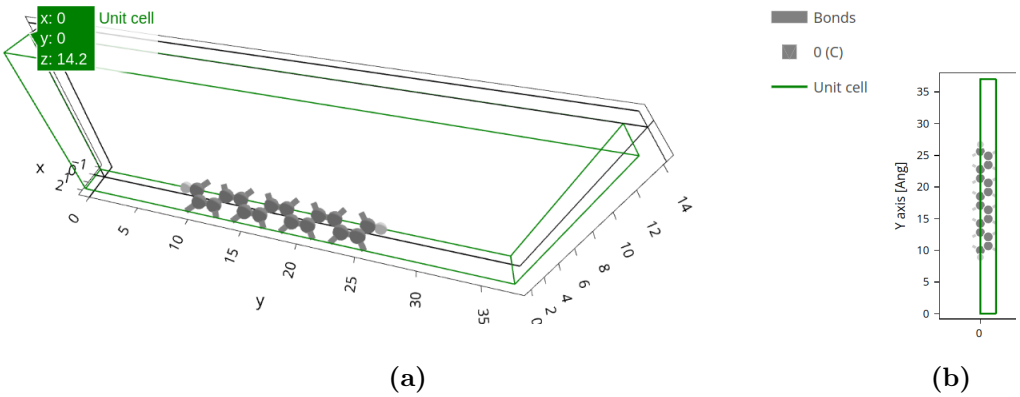

(a) **(b)**

Figure 1: Graphical representation of the ZGNR unit cell inputted to SIESTA. In (a) the 3D cell is represented, while in (b) its 2D projection. The two C atoms in the edges are labeled as 0 and 7 (we will call them R and L).

Listing 2: Routines employed to generate the configuration files and run SIESTA from Python for all the executions of the present work.

```python
import numpy as np
import sisl
import os
from Pseudopotential_file_generator import *

def prepare_SIESTA_inputs(geometry, exp_name, output_path, basis_size='DZP', Nkx=10, Nky=1,
            Nkz=1, saveH=True, saveRho=True, relaxation=False, maxForceTotal=0.01,
            maxSteps=1000, spin_polarized=False, particular_spins={0:[1, 0, 0], 3:[-1, 0,0]},
            electric_field=None, save_total_potential=False, use_DM=False, take_DM_from=None,
                        ):
    out_dir = output_path+f"{exp_name}_Basis_{basis_size}_Nkx={Nkx}_Nky={Nky}_Nkz={Nkz}/"
    os.makedirs(out_dir, exist_ok=True)

    # generate pseudopotential files
    generate_C_psf(out_dir+"/C.psf")
    generate_H_psf(out_dir+"/H.psf")
    # generate the initial ansatz geometry file
    geometry.write(out_dir+ "/geom.fdf")

    # Inside this directory, open a RUN.fdf file, as our main input file.
    with open(out_dir+ '/RUN.fdf', 'w') as f:
        # We include the fdf file that contains the geometry, with the %include statement
        f.write("%include geom.fdf \n")
        # the basis size and basis parameter input.
        f.write(f"PAO.BasisSize {basis_size}\n")
        f.write("DM.MixingWeight  0.100\nDM.NumberPulay  3\n")
        if saveH:
            # We want the converged Hamiltonian to be saved
            f.write("TS.HS.Save true\n")
        if saveRho:
            # Save the electronic density
            f.write("SaveRho true\n")
        # Define the employed k-space grid
        k_grid=f"%block kgrid.MonkhorstPack\n{Nkx} 0 0  0\n 0 {Nky} 0  0\n   0 0 {Nkz}  0\n%endblock kgrid.MonkhorstPack\n"
        f.write(k_grid)
        if relaxation:
            # Conjugate gradient minimization for geometry relaxation
            #   SIESTA will compute the convergent electronic states with the siesta algorithm
            #   at each iteration of the geometry relaxation
            f.write("MD.TypeOfRun CG\n")
            # stopping criterion, if max force on atoms is this, stop
            f.write(f"MD.MaxForceTol {maxForceTotal} eV/Ang\n")
            # maximum steps, if convergence not achieved at this number of steps
            #   stop the search
            f.write(f"MD.Steps {maxSteps}\n") # maximum steps
        if spin_polarized:
            # set spin polarized calculation
            f.write("Spin polarized\n")
            if particular_spins is not None:
                f.write("%block DM.InitSpin\n")
                for k,v in particular_spins.items():
                    f.write(f"{k} {v[0]} {v[1]} {v[2]}\n")
                f.write(f"%endblock DM.InitSpin\n")
        if electric_field is not None:
            f.write(f"%block ExternalElectricField\n{electric_field[0]} {electric_field[1]} {electric_field[2]} V/Ang\n%endblock ExternalElectricField\n")
        if save_total_potential:
            f.write("SaveTotalPotential true\n")
        if use_DM:
            os.system(f"cp {take_DM_from}/siesta.DM {out_dir}/siesta.DM")
            # if already a good enough initial density matrix ansatz is available
            f.write("DM.UseSaveDM true\n")
    return out_dir

def run_siesta_on(path_to_run, siesta_path):
    os.system(f"cd {path_to_run}; {siesta_path} RUN.fdf > RUN.out")
```

Now, in order to get a more realistic ribbon as the calculation basis, we run a relaxation round in SIESTA with the code exposed in Listing 2. For all the SIESTA calculations of the work, we decided to employ a k-grid of $(N_x, N_y, N_z) = (10, 1, 1)$, since the transport direction for the ribbon is directed along x and in y, z, only alternative ribbons are extended periodically. $N_x = 10$ was decided to be enough, because we already found the results of the original paper [1] with this. Regarding the basis set, the double-z polarized set is employed. For the relaxation we set no spin polarization nor electric field and set a maximum force tolerance of 0.01 eV/A as convergence criterion (and a maximum of steps in the minimization of 1000). The obtained relaxed structure cannot be distinguished from the one of Figure 1 with the naked eye. However, the total energy of the system did stabilize about 2 eV, from -2615.632498 eV to -2617.078119 eV. The band structure, fat-bands by atoms and projected density of the resulting structure can be found in Figure 2. The band structure is practically the same as the one shown in the original reference [1]. A continuity of states is available around the Fermi level, so we can say that the GZNR seems to be metallic when no spin considerations are taken. Looking at the fat-bands and the density of states, we realize that the states around the Fermi level are mainly due to atoms 0 and 7, which are the ones located in the edges. Those appear to be the ones relevant for transport, as we will confirm in a moment.

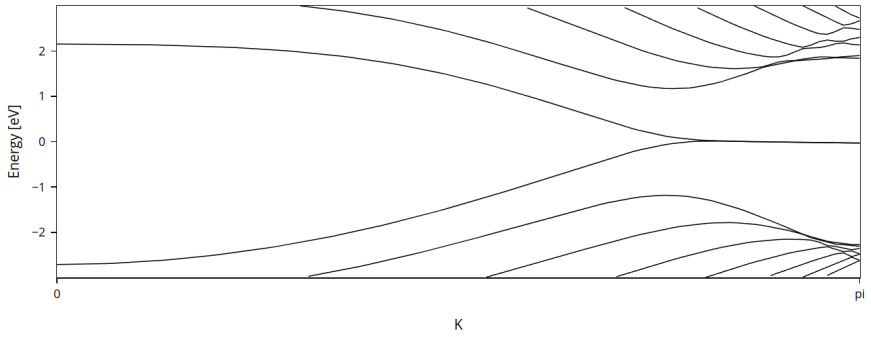

(a) No Spin Polarization - Band Structure

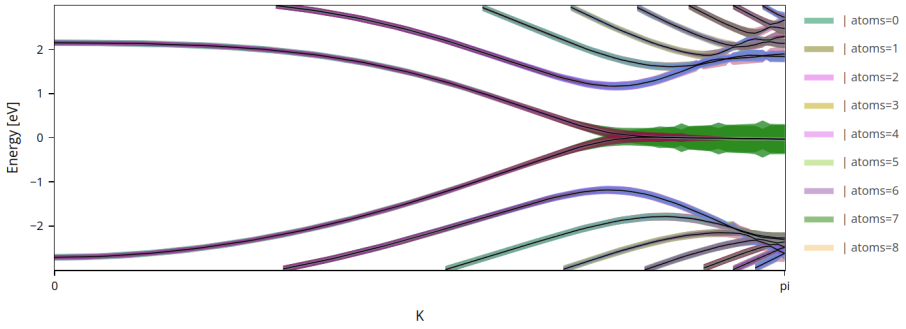

(b) No Spin Polarization - Flat Bands by Atomic contribution - around Fermi level atoms 0,7, the ones in the edges give the main contribution

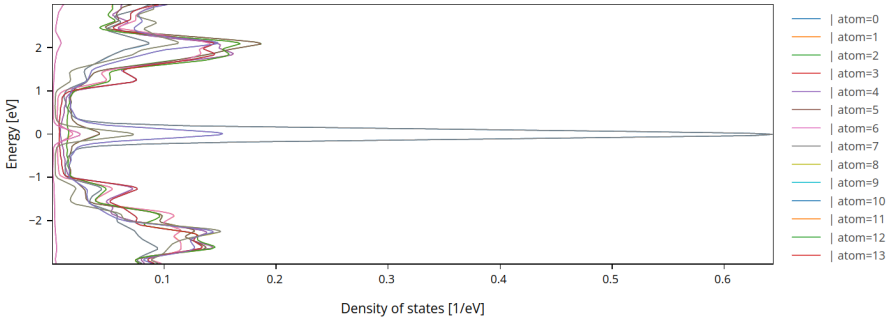

(c) No Spin Polarization - Projected Density of States - Effectively, most states around the Fermi level are due to the atoms in the edges (0 and 7)

Figure 2: Obtained results for **no spin polarization.**

2 ZGNR with Varying Spin Polarization

Because we want to study the conduction properties of the material, we will center our analysis around the Fermi level.

We analyze the band structure of the ZGNR when no electric field is present. For a more realistic calculation than the one resulting from the relaxation we activate spin polarization in the SIESTA calculation. We first run a simulation with an initial configuration in which all spins are aligned, where we find the band-structure plotted in Figure 3.(a). We can see that the result are two copies of the band-structure morphology we found when no spin was considered, but with an energy shift as a function of the spin. To be more precise, we expect for the converged result a graphene-like behaviour in x, because at the Fermi level the degeneracy breaking causes a band-crossing similar to the one found in the Dirac cone [6]. In Figure 4.(a), we see the fat-bands by atomic contribution and find that for all the states around the Fermi level, essentially atoms 0 and 7, the ones in the edges of the ribbon, are the main contributors. Indeed, in Figure 4.(b), after plotting the molecular wavefunctions at $K = (\pi/1, 0, 0)$, either for the two degenerate states closest to the Fermi level from above and from below, we find that only the edges of the ribbon have significantly non-zero values. What is more, this happens symmetrically for the edges and spins (no side appears to prefer a spin orientation). Finally, the projected density of states in Figure 4.(c) confirms this conclusion, now for the whole K-space.

Because we only care about the states near the Fermi level, we now try to see if the system converges to the same structure when only the edges are initialized with aligned spins (leaving unpolarized the rest of atoms). We plot its band-structure in Figure 3.(b), which is indeed essentially the same result obtained after polarizing all atoms. In fact, if we take a glance at the converged structure energies of Table 1, we only find differences at the order of $10^{-3} meV$, suggesting clearly the new initial condition was in practice, equivalent.

Table 1: Converged energies for different intial configurations.

Initial configuration	All aligned	Edges aligned	Edges anti-aligned
Energy (eV)	-2617.128790	-2617.128796	-2617.129309

After the success of only considering the edge spins, we can now try the alternative initial condition of anti-aligned spins at the edges, in order to check that the aligned structure was not just a local minimum. It turns out, by looking at the initially anti-aligned condition's post-convergence energy in Table 1, that it gives an even deeper minimum. The difference is only on the order of $1meV$, but for adequate temperature conditions, we can assume that the ribbon will have mainly the behaviour due to the last configuration. We plot the spin-resolved band structure in Figure 3.(c). First of all, note that the resulting structure is spin degenerate everywhere, unlike what happened in the aligned case. Then, we find a band-gap around the Fermi-level, of about $0.3eV$, which means the material behaves as an insulator (as a semiconductor, better said, but we will omit the difference in this work, for the exact band-gap size will depend on the ribbon width). Now, in Figure 5.(a), we plot the fat-bands for the edge atoms, as a function of the spin, and find a very interesting result. Just below the Fermi-level, the last occupied levels are exclusively made of atom 7 (or L) with an up spin, and atom 0 (or R) with a down spin. Meanwhile, the first levels above the Fermi level are their alternatives. This is confirmed in Figure 5.(b) and (c), where we plot the molecular orbital for the two degenerate states closest to the Fermi level from below, at $K = (\pi/a, 0, 0)$, and find that they are exclusively concentrated (with opposed spins) at the edges of the ribbon. It is noteworthy that even if these levels are energy degenerate for both spins, spatially they represent very differently localized states. Finally, the projected density of states in Figure 5.(c) leads us to the same conclusion, so the result is not only valid for the specific path in K space we selected in the band-structure plots.[1]

[1] All this is in good agreement with the original paper [1]. From their figures, we can see that they directly consider the configuration with edge anti-aligned spins alone. Therefore, in the remaining analysis we will just consider so.

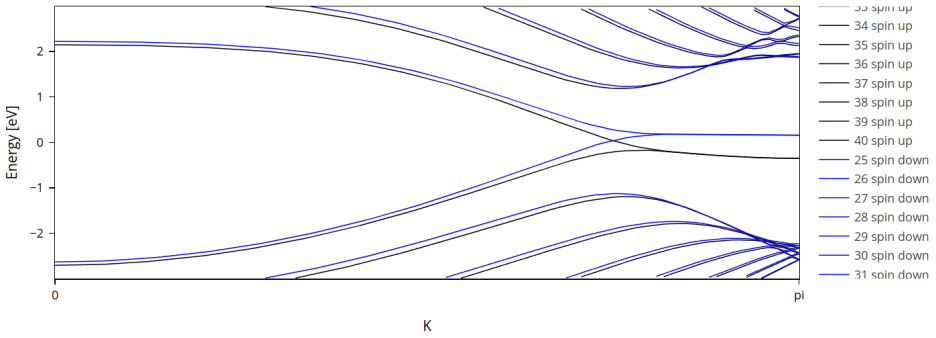

(a) Spin Polarization, all spins aligned initial configuration - Band Structure. Black lines are the band structure for spin up and blue lines are for spin down.

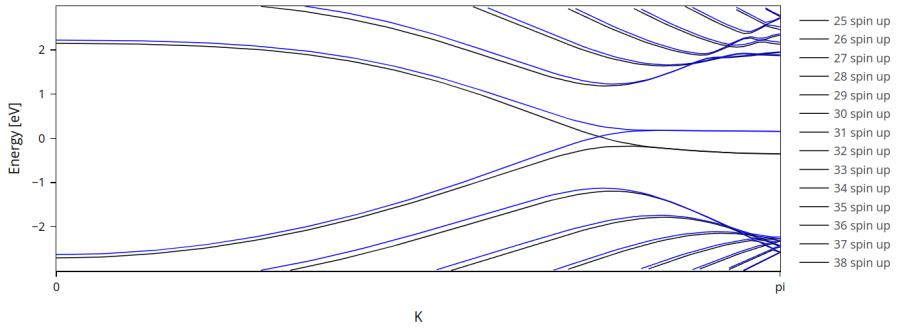

(b) Spin Polarization, edge atom spins aligned initial configuration - Band Structure. Black lines are the band structure for spin up and blue lines are for spin down.

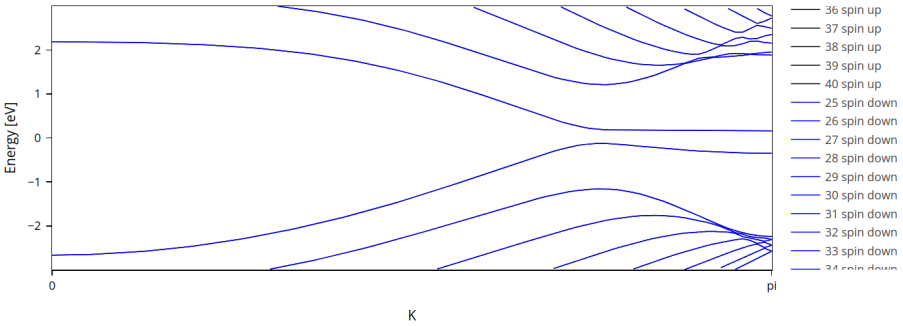

(c) Spin Polarization, edge atom spins anti-aligned initial configuration - Band Structure. Black lines are the band structure for spin up and blue lines are for spin down. Note that the band structure is degenerate for spin up and down.

Figure 3: Obtained results for spin polarization but no electric field. Clearly, only considering the edge spins the result we obtain is the same (see (a),(b)). Note the band gap appearing in (c) when the spin anti-aligned configuration is set.

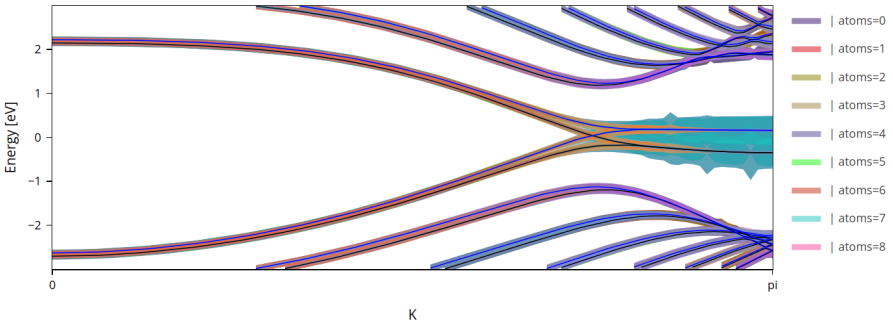

(a) Band Structure with fat-bands by atom contribution.

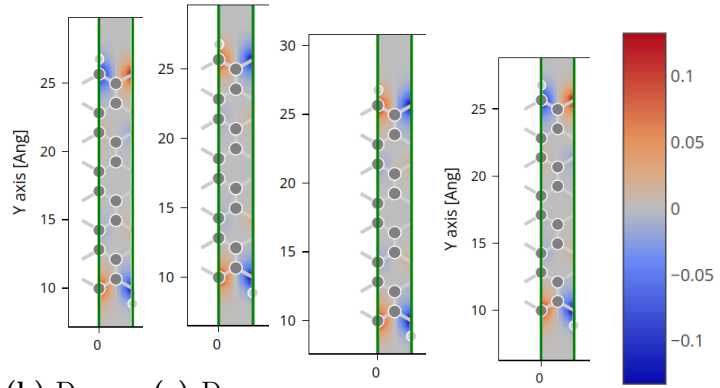

(b) Down 1 **(c)** Down 2 **(d)** Up 1 **(e)** Up 2

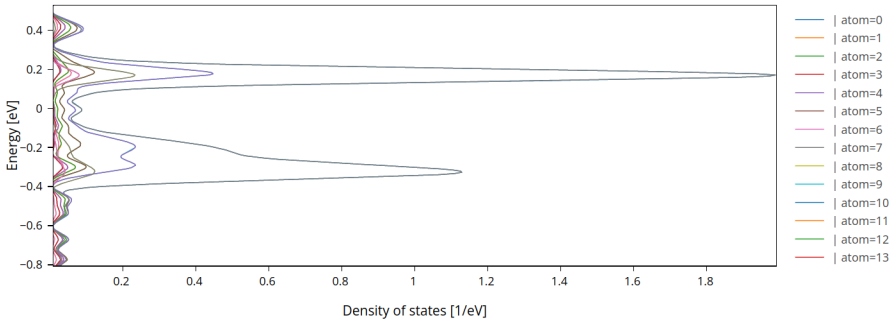

(f) Projected density of states per atom.

Figure 4: Converged results for the **aligned** spin initial configuration. In (a) the band structure can be seen, where fat-bands as a function of contribution per atom are provided. Clearly, the main contributors to the states around the Fermi level are atom 0 and 7, which are the ones in the edges of the ribbon. This is confirmed by (b) and (c), where we can see the (real) molecular wavefunction at $K = \pi(1/a)$ for the two degenerate states closest to the Fermi level but above (having both spin down). These (real) wavefunctions are localized around the edges. The same happens in (d) and (e), where the molecular wavefunction is plotted now for the two degenerate states closest to the Fermi level but below (having both spin up). The scale for all the molecular wavefunctions is the same and is provided after (e). Finally, the projected density of states per atom in (f) shows the same conclusion for the states around the Fermi level.

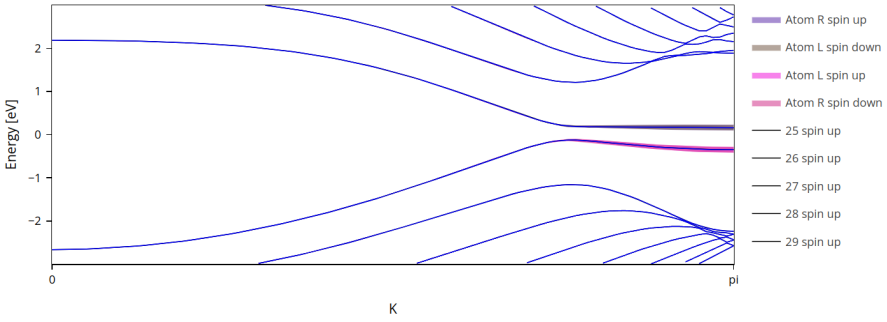

(a) Band Structure with fat-bands by atom contribution.

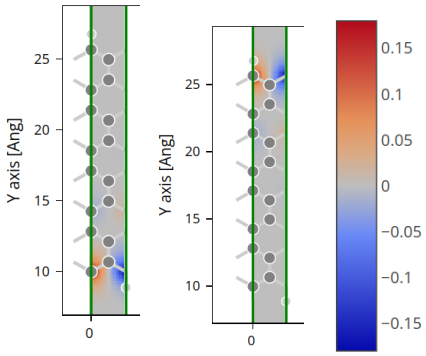

(b) Down **(c)** Up

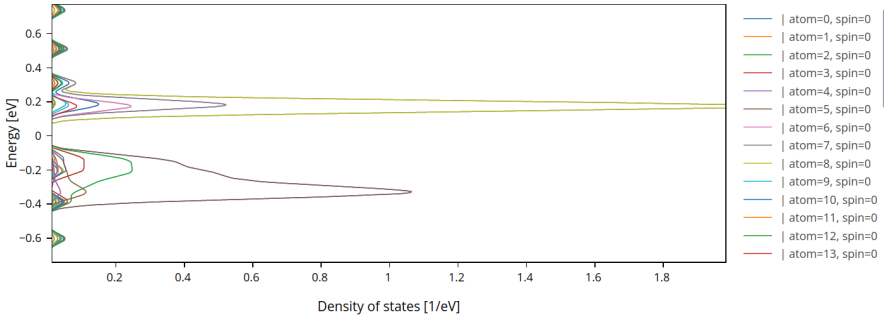

(d) Projected density of states per atom.

Figure 5: Converged results for the anti-aligned spin initial configuration. In (a) the band structure can be seen, where fat-bands for the edge atoms, atom 0 or R and atom 7 or L are provided. We can see that the last energy level below the Fermi level, for spin up is located around atom L, while for spin down it is located around atom R, since these are the main contributors. Indeed, in (b) and (c), we can see the molecular wavefunctions at $K = \pi(1/a)$ for the two closest states to the Fermi level from below. They have spin up and down respectively, and we see that the wavefunction is spatially localized in a single edge of the ribbon in each one of the cases. Thus, the initially anti-aligned configuration has converged into an anti-aligned configuration as the most stable one around the Fermi level. The scale for all the molecular wavefunctions is the same and is provided after (c). Finally, the density of states in (d) gives us the same conclusion.

3 ZGNR with an Electric Field

Finally, for the most stable configuration we found (the one with the edge spins anti-aligned), we run a grid of SIESTA simulations with static electric fields $\vec{E} = (0, E_y, 0)$ along the y-axis, with $E_y \in (0, 0.5)\, eV/A$. The field along the y axis, where we can couple the edges of the ribbon, which had opposed spins, is meant to see if we can introduce any asymmetry in the spin resolved band-structure. We choose the values of E_y following the ones chosen in the original reference [1].

We plot in Figure 7 the spin resolved band structures for 4 increasing field values. Effectively, we achieve an asymmetric band bending for the spins. Most of the band structure still has the spin states degenerated in energy. However, for the proximal ones to the Fermi level, the down spin states see their banned gap monotonously reduced with increasing field, while the up spin states see their banned gap monotnously increased. This is such that by $E_y = 0.5eV/A$, for down spin states, the gap is closed and a fully continous density of states is available (just as in the case when no spin polarization was even considered), giving rise to a metallic behaviour for down spin states. Meanwhile, the gap for the up states increases towards $0.5eV$, increasing the resistivity for up spin states. All these results match perfectly the ones found in the reference [1]. Thus we assert that ZGNR has a prominently half-metallic behaviour (even if we will need to play with the temperature and applied voltages in order to really avoid semiconductivity, or alternatively make the ribbon narrower[2]).

To really see what happens when we increase the field at the level of the edges, and to confirm that the behaviour for the plotted path in K space in the band structures is generalizable to all the material, in Figure 8, we plot the projected density of states as a function of the increasing field. We find that even when the field is applied, the atom in each edge contributes purely to one spin state and that these spins are the opposite (if for atom L spin down is lower in energy, spin up is lower for atom R). Then, as the field increases, we see that while the states around L decrease their energy, the states around R increase in energy. This is because a constant and static electric field implies a linear potential, which leaves the atoms in one edge of the ribbon at a lower potential than those in the other edge, and because the molecular orbitals are localized in the edge atoms, this directly displaces these molecular orbitals in energy, according to the external potential on the atoms.[3] These relative shift on the edge energies, causes that from a certain field on, the up states on atom L and the up states on atom R start to get more and more degenerate, until at a certain point, a continuity of states is available around the Fermi level.

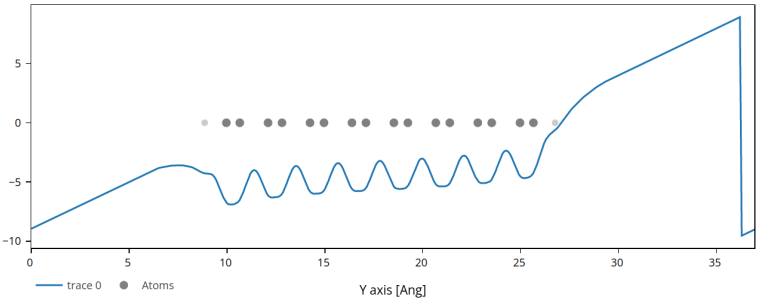

Figure 6: Cross-section in y for the total potential energy profile employed in the SIESTA calculation when $E_y = 0.5eV/A$.

4 Conclusion

We conclude that the obtained results replicate those obtained in Ref. [1], even if we also highlight potential difficulties in the experimental design of half-metallic ZGNR, which might have not been as underlined in the original reference.

[2] A narrower ribbon would make the interaction between the edges stronger, making the gap wider. This would also mean a higher electric field would be necessary to obtain half-metallicity

[3] See Figure 6 for a plot of the total potential energy field employed in the SIESTA calculations for instance for the $E_y = 0.5eV/A$ case.

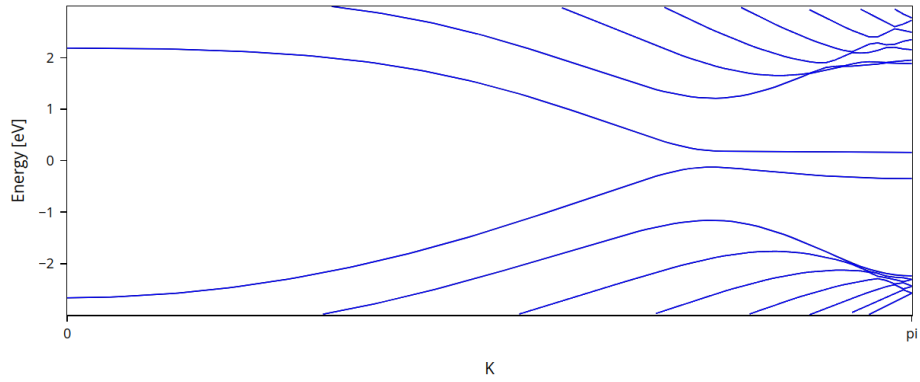

(a) Antialigned Spin Polarization $E_y = 0\,V/A$ - Band Structure - Insulator for both spins

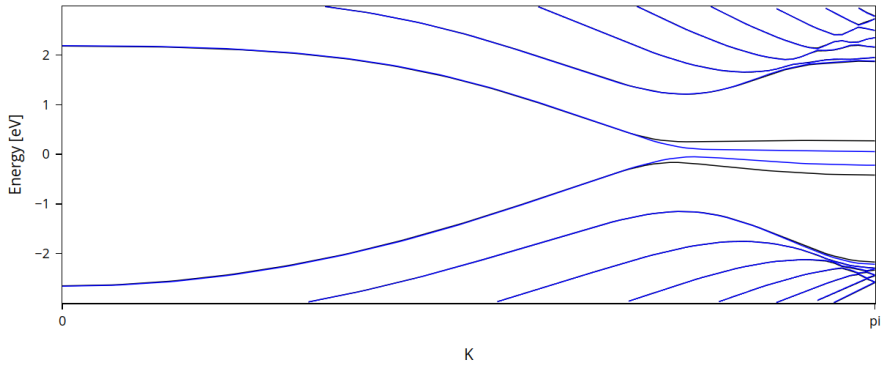

(b) Antialigned Spin Polarization $E_y = 0.1\,V/A$ - Band Structure

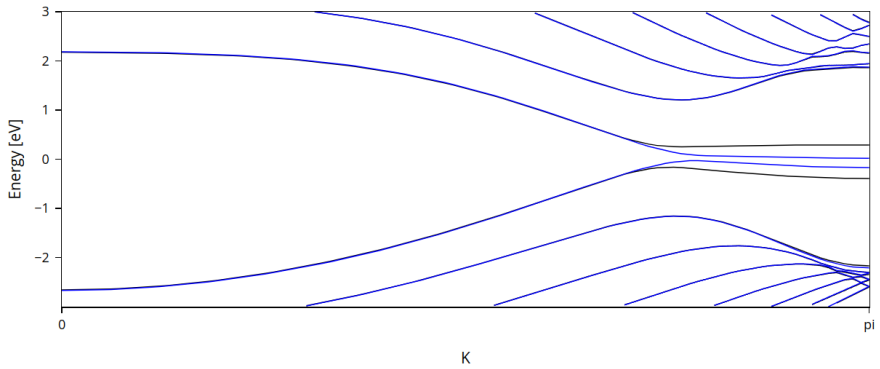

(c) Antialigned Spin Polarization $E_y = 0.2\,V/A$ - Band Structure

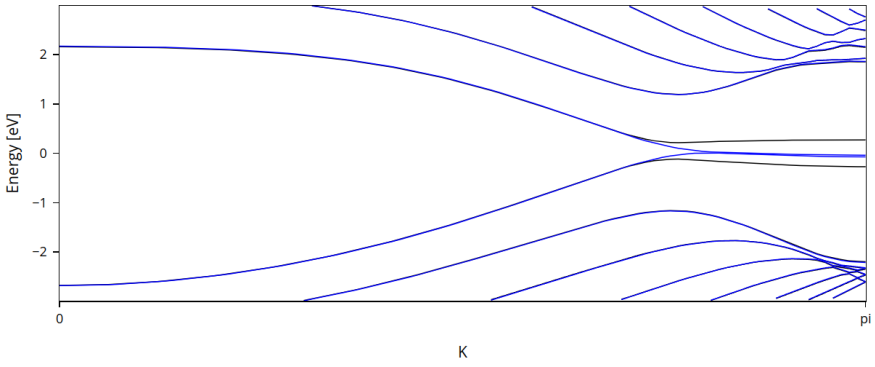

(d) Antialigned Spin Polarization $E_y = 0.5\,V/A$ - Band Structure - Conductor for spin down, insulator for spin up

Figure 7: In black we see the bands for spin up and in blue those for spin down.

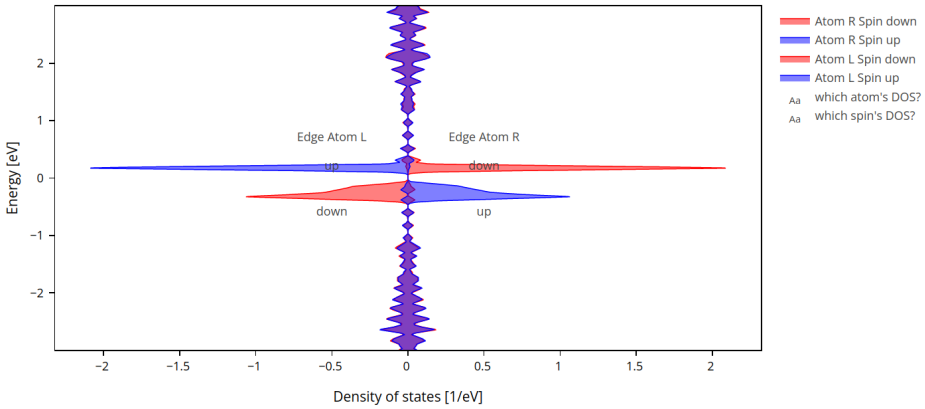

(a) Antialigned Spin Polarization $E_y = 0\,V/A$ - Projected DOS - Insulator for both spins

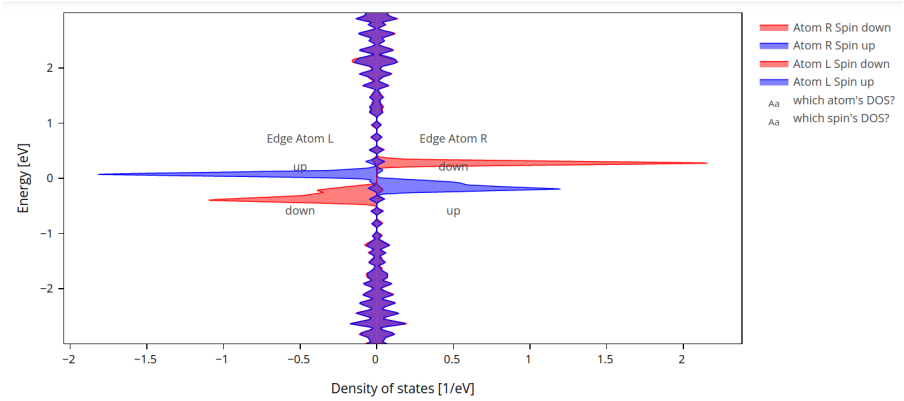

(b) Antialigned Spin Polarization $E_y = 0.1\,V/A$ - Projected DOS

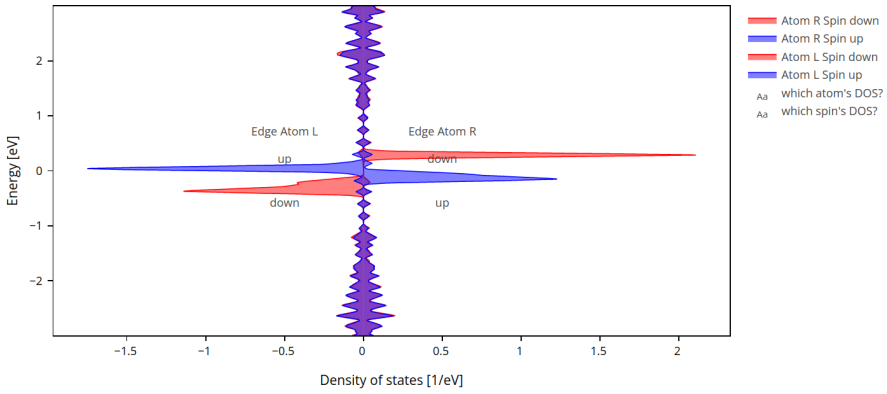

(c) Antialigned Spin Polarization $E_y = 0.2\,V/A$ - Projected DOS

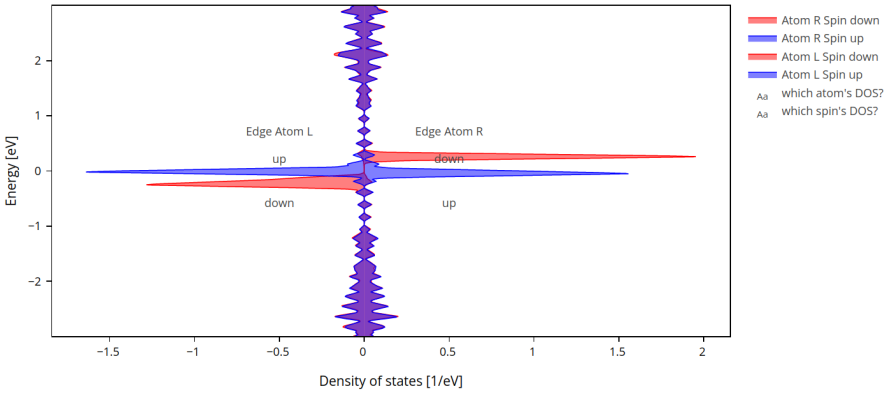

(d) Antialigned Spin Polarization $E_y = 0.5\,V/A$ - Projected DOS - Conductor for spin down, insulator for spin up

Figure 8: In black we see the bands for spin up and in blue those for spin down.

References

[1] Y.-W. Son, M. L. Cohen, and S. G. Louie, "Half-metallic graphene nanoribbons," *Nature*, vol. 444, no. 7117, pp. 347–349, 2006.

[2] J. M. Soler, E. Artacho, J. D. Gale, A. García, J. Junquera, P. Ordejón, and D. Sánchez-Portal, "The siesta method for ab initio order-n materials simulation," *Journal of Physics: Condensed Matter*, vol. 14, no. 11, p. 2745, 2002.

[3] A. García, N. Papior, A. Akhtar, E. Artacho, V. Blum, E. Bosoni, P. Brandimarte, M. Brandbyge, J. I. Cerdá, F. Corsetti, R. Cuadrado, V. Dikan, J. Ferrer, J. Gale, P. García-Fernández, V. M. García-Suárez, S. García, G. Huhs, S. Illera, R. Korytár, P. Koval, I. Lebedeva, L. Lin, P. López-Tarifa, S. G. Mayo, S. Mohr, P. Ordejón, A. Postnikov, Y. Pouillon, M. Pruneda, R. Robles, D. Sánchez-Portal, J. M. Soler, R. Ullah, V. W.-z. Yu, and J. Junquera, "Siesta: Recent developments and applications," *The Journal of Chemical Physics*, vol. 152, no. 20, p. 204108, 2020.

[4] N. Papior, "sisl," 2022.

[5] "Github repository with the python scripts and notebook generated for the report." https://github.com/Oiangu9/_Miscellaneous/tree/main/SSN.

[6] "Wikipedia entry on the driac cone." https://en.wikipedia.org/wiki/Dirac_cone.